A Parameter Study of Low Frequency Two-Body Wave Energy Converters

Xueyu Ji[#1], Elie AI Shami[#2], Xu Wang[#3], Lei Zuo[*4]

[#] *School of Engineering, Royal Melbourne Institute of Technology University, Melbourne, Victoria, Australia*

[3]xu.wang@rmit.edu.au

[*] *Department of Mechanical Engineering, Virginia Polytechnic Institute and State University, Blacksburg, VA 24061, USA*

[4]leizuo@vt.edu

***Abstract*— This paper studies a two-body wave energy converter which is a two-degrees-of-freedom oscillating point absorber. The two-body wave energy converter oscillating in heave with a floating body of variable geometry connected to a submerged body is designed for the Australian ocean wave conditions with excitation frequency ranging from 0.08 Hz to 0.12 Hz and wave height of 1 m. Taguchi method has been applied to investigate the system model parameters' influences on the average power output where the main input variable parameters are the power take-off stiffness and damping coefficients, submerged and floating body geometries, depth of the submerged body, floating body draft, diameter and geometry inclination angle. ANSYS AQWA is employed to obtain the hydrodynamic parameters in the regular wave conditions in order to calculate the output power. Both linear and non-linear dynamic models of the two-body wave energy converter will be analysed and simulated in both the time and frequency domains. The Power-take-off stiffness coefficient and submerged body geometry have been identified to be the most important parameters in influencing the average power output in the studied frequency range.**

***Keywords*— 2 DOF, Point absorber, Taguchi method, Optimization**

I. INTRODUCTION

Wave energy is a prominently renewable energy that is both periodical and predictable. Because of the energy crisis and greenhouse effects, wave energy has been an interesting topic in last few decades. The power contained in wave propagation along the ocean's surface can reach a few Terra-Watts. Average power flow intensity is typically 2–3 kW/m^2 perpendicular to direction of wave propagation, which is much more than the power available from solar (0.1-0.3 kW/m^2) or wind (0.5 kW/m^2) energy [1]. Many proposed devices such as surface attenuator [2], water oscillating columns [3], water overtopping devices [4], and so on are being developed to efficiently harvest the energy contained in ocean waves. However, none of them has really stood out as a definitive choice of a wave energy-harvesting device to be developed commercially and connected to power grids around the world. Apart from that, the point absorber, which makes use of the resonant effect when coupled with a linear generator, is considered as an interesting option to extract energy from waves. It presents low complexity and maintenance and potentially high efficiency. However, due to the low frequency of the energetic ocean waves in regions such as Australia (0.08 Hz to 0.12 Hz near the south) [5], huge mass and volume of a buoy are typically needed in order to push the resonant frequency down and absorb as much energy as possible, which is impractical and costly to realize. A two-body wave energy converter with a submerged body and a floating buoy are adopted for the Australian sea state as it has two degrees of freedom (DOF) which can increase the equivalent mass of the system greatly due to the increase of the hydro-dynamically added mass without a major increase of the physical mass. This increase in the mass results in a reduction of the first natural frequency, thus resulting in the ability to operate at low frequencies. Currently available two body wave energy converters such as Wavebob [6] and Powerbuoy [7] are displayed in Fig. 1. The wave energy converter's (WEC) numerical model has been discussed by Liang (2016) [8] and is shown in Fig. 2, but this model did not take into considerations of the non-linear effects which may exist in the buoy's hydrostatic stiffness (non-uniform shape) or the viscous damping force. The influences of the floating buoy geometry, diameter, draft, damping coefficient, wave height and wave period on the power output have been researched by Amiri (2016) [9], but the viscous damping of the submerged bodies was neglected. Even though a non-linear spherical buoy was proposed by Dai (2015) [10], its non-linear hydrostatic stiffness was not elaborated properly. J. Engström (2011) [11] proposed using a two-body system coupled with a linear driven generator, but the main issue is neglecting the viscous damping in the numerical model based on the assumption that the effects of the viscous damping on the power are very small for a submerged oscillating sphere. Based on the conclusion of Gao (2017) [12], the phase difference between the induced voltage and current leads to the variation of the PTO force: one is linked with the velocity which can be modelled as a damping force and the other one is related to displacement and is modelled as a spring stiffness force. In this paper, the proposed model includes the viscous damping, non-linear effect. The PTO is modelled as a spring damper device. Even though there are many other types of PTO, like hydraulic actuators [13], rack pinion systems [14-15] and hydraulic turbines [16], the linear generator [11] is an outstanding option with high efficiency, simplicity and low maintenance fees. Therefore, a generic linear generator is introduced in this research. The operational conditions in the

ocean are complex. The influence of each parameter is somehow dependent on the other parameters. For example, the sea state determines the geometry, which alters the hydrodynamic coefficient. The hydrodynamic coefficient affects the control algorithm, thus affects the PTO coefficients. Therefore, Taguchi method which has been used to conduct parameter sensitivity studies and optimizations in the chemistry process industry [17] can be helpful to evaluate the influence of the different parameters, as it can analyse the response of the system under the variation of each parameter, and detect the best combination of parameters to produce the highest power.

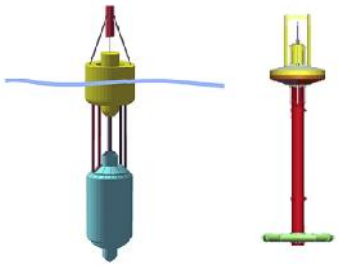

Fig.1 Wavebob and Powerbuoy [8]

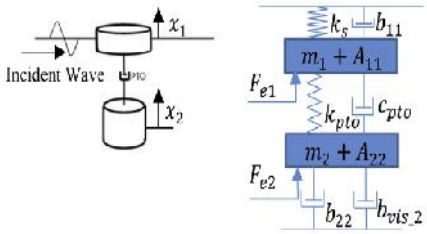

Fig.2 Numerical model of the Wavebob and Powerbuoy [8]

II. TAGUCHI METHOD AND THE VARIABLES

In this paper, seven parameters listed in Table 1 are selected as the input variables. The hydrodynamic parameters such as the added mass, radiation damping, and excitation force are simulated using ANSYS AQWA. Fig. 3 (a) shows the buoy configuration with the variable inclination angle θ and Fig. 3 (b) represents the two-body wave energy converter analysed in this study. The geometries are drawn using a CAD software and the model is deployed in ANSYS AQWA where the regular waves are defined with the frequencies varying from 0.08 Hz to 0.12 Hz (Australian ocean wave frequencies) and a wave height of 1 m. However, due to the limitations of the ANSYS AQWA, the viscous damping is not considered in the solution. ANSYS AQWA is a boundary element method software based on the linear potential wave theory. In order to calculate the viscous damping forces, a software based on the finite volume method such as ANSYS CFX is required. The viscous damping data can be estimated from experimental data in the literature. The variation of the parameters is divided into two levels in Table 1 and eight sets of simulations should be run based on Table 2. The final simulations should be conducted in the frequency and time domain using the Matlab and Matlab Simulink codes. For the time domain analysis, 9 frequency samples with equal frequency interval (0.005 Hz) are selected for the frequency range from 0.08 Hz to 0.12 Hz where the hydrodynamic parameters at each of individual frequencies will be used as inputs of the Matlab Simulink code to get the average power output. Then the nine average power outputs can be utilized to produce an average power vs. frequency curve in frequency domain to find the maximum average power output in the frequency range for the non-linear model.

In Taguchi method, the first parameter is the buoy's inclination angle which generates the linear and non-linear influences on the energy output. The second and seventh parameters are mainly set for studying the influence of the buoy geometry. The submerged body geometry affects the viscous damping and added mass. A shape with high added mass increases the system's inertia but also tends to increase the system's viscous damping, which lowers the captured power. The third parameter is to find the effect of the spherical and cylindrical shapes of the submerged body on the power output. The large added mass of the submerged body can reduce the natural frequency to increase the harvested power in low frequencies but the large viscous damping of a submerged cylinder reduces the captured power. To maintain a consistent size in the heaving direction, radiuses of the submerged body of cylindrical and spherical shapes are set to be 3 m. According to J. Engström (2011) [11], the submerged depth can affect the final power output outcome, if the submerged body is placed deep enough, the hydrodynamic interactions between the two bodies can be avoided. PTO parameters like the damping and stiffness coefficients can have a large effect on the conversion frequency bandwidth [18] and natural frequency, they are presented by Parameters 5 and 6 in Table 1.

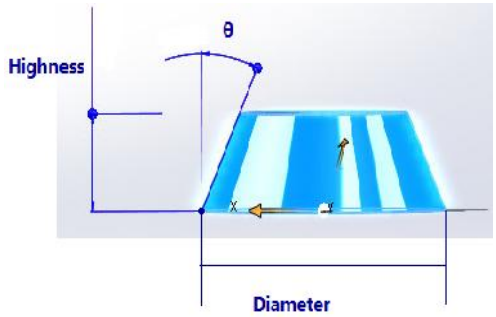

Fig.3 (a) Illustration of the floating buoy parameters

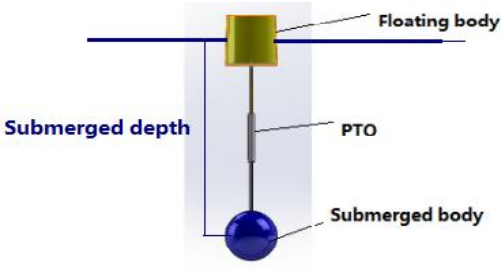

Fig.3 (b) Illustration of the wave energy converter device

III. NUMERICAL MODEL

For the two-body wave energy converter, the submerged body is set to have neutral buoyancy when placed in a stationary wave. In this section, both linear and non-linear models will be elaborated. The added mass, radiation damping, viscous damping and excitation force will be presented in the dynamic equations.

IV. LINEAR MODEL

For the linear model, the buoy is set to have a constant cross section with a zero-inclination angle. The equations of the 2 DOF mass spring dashpot system can be developed based on the model in Fig. 2. The wave excitation forces exerted on the buoy and submerged body are f_{e1} and f_{e2} respectively. Radiation damping of the buoy and submerged body are b_{11} and b_{22} respectively, but b_{22} is ignored since it is very small compared to b_{11}. The added mass for the buoy and submerged body are a_{11} and a_{22} respectively. All these parameters can be obtained via simulations done in ANSYS AQWA. Once the geometry features of the buoy are set, the hydrostatic stiffness k_s can be calculated using Equations (1) and (2). Based on the submerged volume of the buoy and submerged body in water, Archimedes' law can be introduced to calculate the added masses of these two bodies. Stiffness and damping coefficients of the power-take-off k_{pto}, b_{pto}, and the radius of the buoy R are all set in two levels according to Table 1 and Table 2. The dynamic heaving motion equations of the linear model under the regular waves are shown in Equations (3) and (4) which can be implemented for the Laplace transformation and analysed in the frequency domain.

V. NON-LINEAR MODEL

Younesian [19] presented a non-linear numerical model which has been proven to be a valid tool in increasing the extracted power and the non-linear effects can be used to broaden the harvesting frequency bandwidth. Equations (5) and (6) are the governing equations of the system for the oscillation in the heaving direction [19]. Due to the non-linear effects, the model has to be simulated in the time domain and some frequencies are chosen to do the simulations. Similarly, the parameters such as f_{e1}, f_{e2}, b_{11}, a_{11}, a_{22} are calculated using ANSYS AQWA. R, $tan\theta$, k_{pto}, b_{pto} and the relevant parameters are listed in in the settings of the Taguchi method as shown in Table 1.

VI. ANSYS AQWA

ANSYS AQWA uses the Boundary Element Method (BEM) to simulate the wave interaction with WEC and both the radiation and diffraction theories are utilized in this software. The potential flow theory is used with the assumption that the velocity potential is irrotational and incompressible. In ANSYS AQWA, the frequency is set to vary from 0.08 Hz to 0.12 Hz with 20 frequency sample points in the decided range. The draft of the buoy is set to be half its height and the wave height is set as 1m for all the cases.

TABLE 1TAGUCHI SETTINGS

Setting	**Level.1**	**Level.2**
1.Inclination angle of floating cylinder	0 deg	25 deg
2.Cylinder draft	1 m	2 m
3.Submerged body geometry	Cylinder	Sphere
4.Submerged depth	20 m	30 m
5.b_{pto}	100000 kg/s	50000 kg/s
6.k_{pto}	100000 N/m	50000 N/m
7.Diameter of the floater	4 m	6 m

$$f_d = \circ \times g \times \circledR \times R^2 \times x_1 \tag{1}$$

$$k_s = \circ\, g\, \circledR\, R^2 \tag{2}$$

$$(m_1 + a_1(\infty)) \times \ddot{x}_1 + \int_{-\infty}^{t} k(t - \tau) \cdot \dot{x}_1(\tau)\, d\tau + b_{vis} \times \dot{x}_1 + \circ g \circledR R^2 \times x + b_{pto}(\dot{x}_1 - \dot{x}_2) + k_{pto}(x_1 - x_2) = f_{e1} \tag{3}$$

$$(m_2 + a_2(\infty)) \times \ddot{x}_2 + b_{pto}(\dot{x}_2 - \dot{x}_1) + k_{pto}(x_2 - x_1) = f_{e2} \tag{4}$$

where R is the radius of the stationary buoy on the ocean surface; x_1, x_2 are the displacements of the buoy and submerged body respectively, f_d is the hydrostatic force of the buoy, g is the gravitational acceleration, $\circ$ is the density of ocean water, b_{vis} is the viscous damping coefficient of the submerged body, m_1, m_2 are the masses of the buoy and submerged body respectively, k_s is the hydrostatic stiffness;

$$(m_1 + a_1(\infty))\ddot{x}_1 + \frac{°g®}{3}\left(\frac{6Rx_1^2}{\tan(90 - -)} + 3R^2x_1 + \frac{4x_1^3}{\tan^2(90 - -)}\right) + \int_{-\infty}^{t} k(t - ²)\cdot\dot{x}_1(²)d² + k_{pto}(x_1 - x_2) + b_{pto}(\dot{x}_1 - \dot{x}_2) = f_{e1} \quad (5)$$

$$(m_2 + a_2(\infty))\ddot{x}_2 + k_{pto}(x_2 - x_1) + b_{pto}(\dot{x}_2 - \dot{x}_1) + b_{vis}\dot{x}_2 = f_{e2} \quad (6)$$

where θ is the inclination angle.

VII. MATLAB SIMULATION

To run the Matlab simulation in the frequency domain, the viscous damping is linearized for the linear models according to Equations (7) and (8). Since the radius is the same in the heaving direction, the characteristic radius is 3 m. From Equations (9), it can be found that the maximum linearized viscous damping coefficient b_{vis} for the submerged body of both a spherical and cylindrical shapes are 1457kg/s and 9107 kg/s respectively.

$$F_d = \frac{1}{2} \times ° \times C_d \times A \times V^2 \quad (7)$$

$$F_d = b_{vis} \times V \quad (8)$$

$$b_{vis} = \frac{1}{2} \times ° \times C_d \times A \times V \quad (9)$$

where the ° is the density of the ocean water, 1025 kg/m^3, the C_d is the drag coefficient set as 0.16 for a sphere and 1 for a cylinder, A is the characteristic area which is 28.274m^2. In the linearized model, V is set to be 0.6283m/s which is the maximum oscillating velocity in the heaving direction.

All the parameters simulated in ANSYS AQWA should be imported into the Matlab. The output power at a certain frequency is calculated by using Equations (3)-(6). The discrete output power values at different frequency points are used to generate the output power spectrum curves through the least square fit method. For the linear model, the maximum average power output in the frequency range of 0.08-0.12 Hz can be simulated and obtained by utilizing Equation (10) [8] in the frequency domain via the Fourier transform. Since the Fourier transform cannot be implemented for non-linear model and therefore the non-linear model simulation has to be conducted in time domain.

For this research, the Matlab Simulink (fixed time step 0.01 and using Runge-Kutta to solve) is applied to conduct the time domain simulation and the average power output in time domain for each frequency can be obtained by Equation (11). In Fig.4, the x axis coordinates of red star points imply the selected ocean wave frequency simulated in time domain in Simulink and y axis coordinates of red star points indicate the average power output at related frequency. The fitting average power curves of the Taguchi simulation groups using the non-linear model are shown in Fig. 4. In this research, the maximum power output values of the fitting average power frequency spectrum curves of non-linear models and the peak average power output of linear model in frequency domain are listed in Table 2. From Table.1, every setting has level 1 and level 2 and for each group in Table.2, it consists of seven settings and the number 1 or 2 of the settings coincides with level 1 and level 2. Apart from that, it can be noticed for each setting, the numbers of level 1 and level 2 are identical. In Table.2, each row manifests a WEC which is comprised of seven controllable parameters with value either level 1 or 2 corresponding with the description in Table.1 and the maximum average output for it will be presented at the right side.The average power output of a specific level of a setting (Average 1 or Average 2) is calculated by summing the output power of all the simulation groups under the same column of the specific setting at the same level and dividing it by 4 as shown in Equation (22). The effect of the setting can be found via the subtraction of the average power value of Level 2 from that of Level 1(Average 2 minus Average 1) using Equation (23). Typically, the large difference means that parameter has a large effect on the average power output.

$$P_{ave} = \frac{1}{T}\int_0^T P_{sim}\,dt = \frac{b_{pto}\,\mu^2}{2}\cdot|X_1 - X_2| \quad (10)$$

$$P_{ave} = \frac{1}{T}\int_0^T P_{sim}\,dt = \frac{1}{T}\int_0^T b_{pto} \times (\dot{x}_1 - \dot{x}_2)^2\,dt \quad (11)$$

where $P_{sim}(t)$ is the simultaneous power generated by the PTO, X_1, X_2 are the magnitude of displacements of the buoy and submerged body, μ is angular frequency.

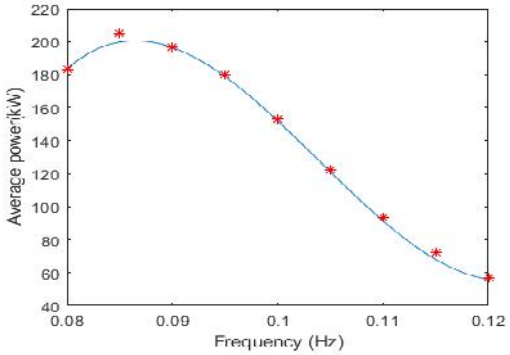

Fig.4 (a) Group 5 average power fitting curve

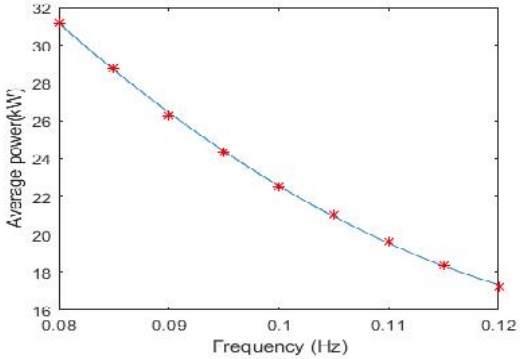

Fig.4 (b) Group 6 average power fitting curve

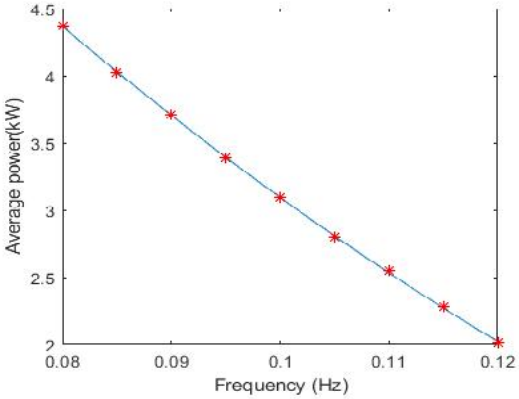

Fig.4 (c) Group 7 average power fitting curve

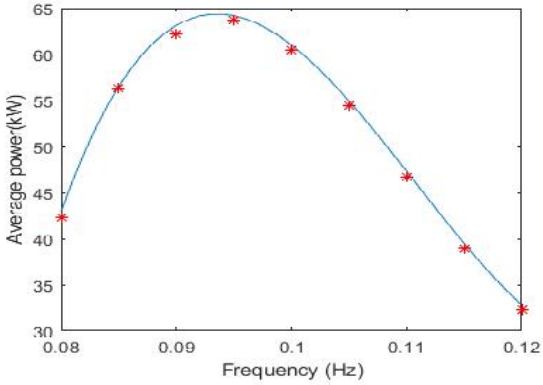

Fig.4 (d) Group 8 average power fitting curve

$$AP_n = \frac{\sum_{i=1}^{4} P_{avg,i}}{4} \tag{12}$$

$$Effect = AP_2 - AP_1 \tag{13}$$

where $P_{avg,i}$ indicates one time-average power output of a simulation group for a special level and for a specific setting variable. AP_n is the averaged power output of all the groups for a special level and for a specific setting variable.

TABLE.2 DATA SHEET

Input variable	Angle	Draft	Submerged geometry	Submerged Depth	b_{pto}	k_{pto}	Diameter of floater	Output
	1	2	3	4	5	6	7	Average (kW)
Settings								
Group 1	1	1	1	1	1	1	1	76.92
Group 2	1	1	1	2	2	2	2	36.81
Group 3	1	2	2	1	1	2	2	65.15
Group 4	1	2	2	2	2	1	1	139.33
Group 5	**2**	**1**	**2**	**1**	**2**	**1**	**2**	**204.65**
Group 6	2	1	2	2	1	2	1	31.2
Group 7	2	2	1	1	2	2	1	4.37
Group 8	2	2	1	2	1	1	2	64.35
Average 1 (kW)	79.55	87.40	45.61	87.77	59.41	121.31	62.96	
Average 2 (kW)	76.14	68.30	110.08	67.92	96.29	34.38	92.74	
Effect (kW)	-3.41	-19.1	64.47	-19.85	36.88	-86.93	29.78	

VIII. DISCUSSION

From Table 2, it can be noticed that the submerged geometry (marked in red) and the PTO's stiffness coefficient (marked in blue) have the effect of 64.47 and -86.93 respectively and are most prominent two parameters in influencing the power output. The positive 64.47 kW means from Level 1 of the submerged body of the cylinder shape to Level 2 of the submerged body of the sphere shape, the output power increases by 64.47 kW. The negative 86.93 kW means from Level 1 of the PTO stiffness of 100,000 N/m being reduced to Level 2 of the PTO stiffness of 50,000 N/m, the output power decreases by 86.93 kW.

The third important influencing parameter is the damping coefficient of the PTO. The fourth important influencing parameter is the diameter of the floater. The effects of the remaining parameters on the average output power are quite similar and small. But the inclination angle parameter which influences the linearity of the numerical model has the least effect of -3.41 kW on the power output. When the inclination angle increases from 0 degree to 25 degrees, the output power decreases by 3.41 kW. The inclination angle of the buoy is considered to affect the hydrostatic force. If the hydrostatic force is increased through the increment of the wave height, the effect of the hydrostatic force could be more prominent and could play a more important role in determining the average power output.

As predicted, the shape of the submerged body has a significant effect on the time averaged power output of the WEC. The large viscous damping dissipates the kinetic energy and hence reduces the average power output. The added masses heavily increase the total masses and enable the WEC to resonate at a low ocean wave frequency.

For a linear model, the natural frequency is coupled with the K_{pto} and mass of WEC. Thereby, if the increase of the WEC mass is much larger than that of K_{pto}, then it may lead to the reduced natural frequency of WEC being less than 0.08Hz. If the increase of the WEC mass is less than that of K_{pto}, it may result in the increased natural frequency of WEC being larger than 0.12Hz. For both the situations, increase of K_{pto} will decrease the maximum average power output in the defined frequency range, consequently the negative effect is shown in Table 2.

For the buoy diameter and draft, the similar effects of 29.78 and -19.1 kW respectively on the average power output can be found. Increasing the diameter of the floater from 4 m to 6 m will increase the output power by 29.78 kW. Increasing the draft of the floater from 1 m to 2 m will decrease the output power by 19.1 kW. These two parameters can affect the hydrodynamic parameters such as the radiation damping, added mass and excitation force. In addition, the added masses and hydrostatic stiffness can also be determined by these two parameter settings. Consequently, it can affect the natural frequency of the linear model. If the natural frequency is in the excitation wave frequency range, the average power output will be high and if the natural frequency is out of the range then the average power output will be low. This is why these two parameters are affecting the average power output. b_{pto} having the effect of 36.88 kW is another parameter that can affect the natural frequency. Decreasing the damping coefficient from 100,000 kg/s to 50,000 kg/s will increase the output power by 36.88 kW. If the reduction of this parameter is large enough, the average power output as well as the relative motion of the buoy and the submerged body will be increased. The submerged depth having the effect of -19.85 kW impacts slightly on the average power output which has verified J.Engström's statements [11] that increasing the submerged depth can also reduce the power output. This is because the submerged depth can influence the magnitude of the wave excitation force of the submerged body and thereby affect the relative motion.

From all the groups of simulation, it can be found that Group 5 produces the maximum average power output of 204.35 kW among all the groups. The optimized parameters of Group 5 are: 1) the inclination angle of the floating cylinder body of 25 degree; 2) the floating cylinder body draft of 1 m; 3) the submerged geometry of sphere; 4) submerged depth of 20 m; 5) the damping coefficient of the PTO of 50000 kg/s; 6) the PTO stiffness coefficient of 100000 N/m; 7) the diameter of the cylinder floater of 6 m. Since all the parameters are affecting each other, it is unlikely to identify the other options to get a better result. Therefore, it can be claimed in all the parameter settings of Table 2, Group 5 is the best choice.

IX. CONCLUSION

The two-body oscillating wave energy converter has been analyzed by varying seven different system model parameters using the Taguchi method. ANSYS AQWA has been used in finding the hydrodynamic parameters for the different parameter groups. Based on the frequency and time domain simulations using the Matlab codes, the maximum average power output can be calculated for the linear and non-linear models in the frequency range from 0.08 to 0.12 Hz in the Australia ocean area. It can be found that the PTO stiffness coefficient and submerged body geometry have the most significant effects on the average power output. The parameter combination group with the best performance among the designed eight simulation groups is Group 5. Even though the effect of the buoy inclination angle is not so prominent in this research, it is still necessary to conduct the further research. Because this paper mainly compares the average power output within the frequency range from 0.08 Hz to 0.12 Hz. More

efforts should be made in investigating the effect of the model parameters on the energy harvesting frequency bandwidth and overall harvesting performance of the proposed WEC system in the Australia sea state. It is also necessary to reduce the viscous damping and optimize the geometry of the submerged body in order to achieve the best WEC energy harvesting performance in the desired operating frequency range.

References

[1] Falnes. J. (2007) “A Review of Wave-energy Extraction”. Marine Structures (2007), 20(4), 185–201.

[2] http://www.esru.strath.ac.uk/EandE/Web_sites/14-15/Wave_Energy/attenuator.html

[3] https://en.wikipedia.org/wiki/Oscillating_Water_Column

[4] http://www.emec.org.uk/marine-energy/wave-devices/

[5] S. J. Illesinghe, et al. "Idealized design parameters of Wave Energy Converters in a range of ocean wave climates." International Journal of Marine Energy (2017).

[6] W. Dick, 2005 U.S. Patent No. 6,857,266. Washington, DC: U.S. Patent and Trademark Office.

[7] http://www.oceanpowertechnologies.com/

[8] C. Liang and L. Zuo. "On the dynamics and design of a two-body wave energy converter." Renewable Energy 101 (2017): 265-274.

[9] A. Amiri, P. Roozbeh and R. Soheil, "Parametric study of two-body floating-point wave absorber." Journal of marine science and application 15.1 (2016): 41-49.

[10] Y. Dai, Y. Chen, and L. Xie. "A study on a novel two-body floating wave energy converter." Ocean Engineering 130 (2017): 407-416.

[11] J. Engström, et al. "A resonant two body system for a point absorbing wave energy converter with direct-driven linear generator." Journal of applied physics 110.12 (2011): 124904.

[12] Y. Gao, et al. "A fully floating system for a wave energy converter with direct-driven linear generator." Energy 95 (2016): 99-109.

[13] C. J. Cargo, et al. "Determination of optimal parameters for a hydraulic power take-off unit of a wave energy converter in regular waves." Proceedings of the Institution of Mechanical Engineers, Part A: Journal of Power and Energy 226.1 (2012): 98-111.

[14] M. F. López, P. Taveira and P. Rosa-Santos. "Numerical modelling of the CECO wave energy converter." Renewable Energy (2017).

[15] C. Liang, A. Junxiao and L. Zuo. "Design, fabrication, simulation and testing of an ocean wave energy converter with mechanical motion rectifier." Ocean Engineering 136 (2017): 190-200.

[16] http://reneweconomy.com.au/worlds-first-grid-connected-wave-energy-array-switched-on-in-perth-77510/

[17] G. Taguchi (1993). Taguchi on robust technology development : Bringing quality engineering upstream (ASME Press series on international advances in design productivity). New York: ASME Press.

[18] G. Tampier and L. Grueter. "Hydrodynamic Analysis of a Heaving Wave Energy Converter." International Journal of Marine Energy (2017).

[19] Younesian, Davood, and Mohammad-Reza Alam. "Multi-stable mechanisms for high-efficiency and broadband ocean wave energy harvesting." *Applied Energy* 197 (2017): 292-302.

[20] Cheng, Z., Yang, J., Hu, Z. and Xiao, L., 2014. Frequency/time domain modeling of a direct drive point absorber wave energy converter. *Science China Physics, Mechanics and Astronomy*, *57*(2), pp.311-320.

[21] https://wikiwaves.org/Ocean-Wave_Spectra

[23] Vicente, P.C., Falcão, A.F. and Justino, P.A., 2013. Nonlinear dynamics of a tightly moored point-absorber wave energy converter. *Ocean engineering*, *59*, pp.20-36.

[20] Falnes, J., 1995. On non-causal impulse response functions related to propagating water waves. *Applied Ocean Research*, *17*(6), pp.379-389.